Available online at www.sciencedirect.com
ScienceDirect
International Journal of Heat and Fluid Flow 29 (2008) 83–93
International Journal of HEAT AND FLUID FLOW
www.elsevier.com/locate/ijhff

Parallel and non-parallel laminar mixed convection flow in an inclined tube: The effect of the boundary conditions

A. Barletta *

Università di Bologna, Dipartimento di Ingegneria Energetica, Nucleare e del Controllo Ambientale (DIENCA), Laboratorio di Montecuccolino, Via dei Colli 16, Bologna I-40136, Italy

Received 29 October 2006; received in revised form 29 April 2007; accepted 19 July 2007
Available online 27 September 2007

Abstract

The necessary condition for the onset of parallel flow in the fully developed region of an inclined duct is applied to the case of a circular tube. Parallel flow in inclined ducts is an uncommon regime, since in most cases buoyancy tends to produce the onset of secondary flow. The present study shows how proper thermal boundary conditions may preserve parallel flow regime. Mixed convection flow is studied for a special non-axisymmetric thermal boundary condition that, with a proper choice of a switch parameter, may be compatible with parallel flow. More precisely, a circumferentially variable heat flux distribution is prescribed on the tube wall, expressed as a sinusoidal function of the azimuthal coordinate ϑ with period 2π. A $\pi/2$ rotation in the position of the maximum heat flux, achieved by setting the switch parameter, may allow or not the existence of parallel flow. Two cases are considered corresponding to parallel and non-parallel flow. In the first case, the governing balance equations allow a simple analytical solution. On the contrary, in the second case, the local balance equations are solved numerically by employing a finite element method.

Keywords: Mixed convection; Non-axisymmetric heat flux; Laminar flow; Parallel flow; Inclined duct

1. Introduction

The subject of laminar mixed convection in vertical or inclined ducts deserves a special interest for its applications in the design of cooling systems for electronic devices or for solar collectors. Several authors have presented theoretical or experimental investigations most of which have been reviewed, for instance, in Aung (1987). The literature of the last decades includes many papers presenting theoretical investigations of buoyancy-induced flows in vertical or inclined ducts. Some of these papers (Lavine, 1988; Barletta and Zanchini, 1999, 2001; Chamkha et al., 2002; Bühler, 2003; Weidman, 2006; Magyari, 2007) describe analytical solutions with reference to fully developed parallel flows. In fact, parallel flow represents the condition that allows a drastic simplification of the governing balance equations, thus giving a chance to find exact solutions at least for the simpler geometries: parallel plane channel, circular or annular duct, rectangular duct. However, if one deals with inclined ducts, the condition of parallel flow can be considered as an exception rather than a rule. This conclusion is a direct consequence of the observation that, in an inclined duct, the buoyancy force vector has a non-vanishing projection on the plane of the duct cross-section. In the fully developed region, the transversal components of the buoyancy force are normally responsible for the onset of a secondary flow that makes velocity a non-parallel helicoidal vector field. It must be pointed out that, in this reasoning, geometry matters. In fact, for a parallel plane channel, parallel flows are still possible when the channel is inclined, for the more commonly employed thermal boundary conditions (Lavine, 1988; Barletta and Zanchini, 2001). For different geometries of the duct cross-section, as circular, annular or rectangular, this is not true.

* Tel.: +39 051 6441703; fax: +39 051 6441747.
E-mail address: antonio.barletta@mail.ing.unibo.it

0142-727X/$ - see front matter © 2007 Elsevier Inc. All rights reserved.
doi:10.1016/j.ijheatfluidflow.2007.07.008

Nomenclature

a	dimensionless function, Eq. (10)
A	function of X and Y, Eq. (9)
b	dimensionless constant, Eq. (10)
B	constant, Eq. (9)
$\mathbf{g}$	gravitational acceleration
g	modulus of the gravitational acceleration
Gr	Grashof number, Eq. (10)
k	thermal conductivity
Nu	Nusselt number, Eq. (38)
P	difference between the pressure and the hydrostatic pressure
Pr	Prandtl number, Eq. (10)
$q_w(\vartheta)$	incoming wall heat flux, Eq. (2)
q_0	constant wall heat flux, Eq. (2)
r	dimensionless radial coordinate, Eq. (10)
R	radial cylindrical coordinate
R_0	duct radius
Re	Reynolds number, Eq. (10)
T	temperature
T_0	average temperature in a duct cross-section, Eq. (11)
u	dimensionless axial velocity component, Eq. (10)
$u_1(r)$, $u_2(r)$	dimensionless functions of r, Eq. (23)
U_z	axial velocity component
U_0	average velocity in a duct cross-section, Eq. (12)
$\mathbf{U}$	velocity
$\mathbf{u}'$	dimensionless 2D velocity vector, Eq. (10)
x, y	dimensionless Cartesian coordinates, Eq. (10)
X, Y, Z	Cartesian coordinates
$\mathbf{Y}$	unit vector in the Y-direction

Greek symbols

α	thermal diffusivity
β	coefficient of thermal expansion
ε_k	dimensionless kinetic energy of secondary flow, Eq. (42)
ϑ	angular cylindrical coordinate
Θ	dimensionless temperature, Eq. (10)
Λ	dimensionless parameter, Eq. (33)
μ	dynamic viscosity
ν	kinematic viscosity
ξ	dimensionless switch parameter, Eq. (2)
ϱ	mass density
ϱ_0	mass density at temperature T_0
φ	tilt angle of the duct axis
Ω	dimensionless parameter, Eq. (33)

Superscripts, Subscripts

$'$	2D vector obtained by projection in the (X, Y)-plane
max, min	maximum, minimum value in a duct cross-section

In a recent paper (Barletta, 2005), a criterion to establish whether parallel flow in an inclined duct is possible or not has been discussed. This criterion is in fact a necessary condition for parallel flow and, as such, precludes the possibility of a parallel velocity field when it is not fulfilled. In Barletta (2005), it is shown that parallel flow is possible only if the temperature gradient, the unit vector in the axial direction and the gravitational acceleration are everywhere coplanar vectors. The necessary condition is tested in the case of a parallel plane channel, showing that the widely studied boundary condition of isothermal walls with unequal temperatures is compatible with parallel flow. However, the compatibility holds only if the channel is tilted in the direction orthogonal to the boundary planes. If, on the other hand, the channel is tilted in the direction parallel to the boundary planes, no parallel flow is possible (Barletta, 2005).

The aim of the present paper is to extend the analysis presented in Barletta (2005), in order to show that proper thermal boundary conditions may allow the onset of parallel flow also for duct geometries different from the parallel plane channel. Reference is made to an inclined circular tube. The prescribed boundary condition is a simple non-axisymmetric thermal boundary condition, namely a wall heat flux sinusoidally varying in the angular direction. In linear cases, this boundary condition yields what can be considered a *fundamental solution* for the analysis of non-axisymmetric flows by means of Fourier series (Barletta et al., 2003). It is shown that the same thermal boundary condition may yield parallel or non-parallel flow depending on the value of a switch parameter that yields a $\pi/2$ rotation in the wall heat flux distribution. In the case of parallel flow, the governing balance equations admit a straightforward analytical solution. In the case of non-parallel flow, a simple analytical solution of the balance equations is not possible and the study is performed numerically by employing a finite element solution procedure. A further objective of the present paper is to extend the criterion for parallel flow discussed in Barletta (2005) and recalled in the next section, in order to include duct flows with an axial temperature change as well as duct flows in a fluid-saturated porous medium. The latter task is accomplished in two short appendices.

2. Necessary condition for parallel flow

Let us analyze mixed convection flow in an inclined duct with an arbitrary cross-sectional shape. Let us choose Cartesian coordinates (X, Y, Z) such that the duct cross-section belongs to the (X, Y)-plane and the Z-axis is parallel

to the duct axis. In other words, the duct cross-section corresponds to a domain $\mathfrak{D}$ in the (X, Y)-plane.

As it has been shown in Barletta (2005), by invoking the validity of the Boussinesq approximation and by assuming that the boundary conditions imply an axially invariant temperature field T, *i.e.* $\partial T/\partial Z = 0$, the following statement holds

> *A parallel flow solution of the local balance equations, i.e. a solution such that* $\mathbf{U}' = 0$, *exists in the fully developed region only if the temperature field is such that* $\mathbf{g}' \times \nabla' T = 0$, *at every position in the domain* $\mathfrak{D}$.

In this statement, symbols $\mathbf{U}'$ and $\mathbf{g}'$ denote the two-dimensional projections on the (X, Y)-plane of the fluid velocity $\mathbf{U}$ and of the gravitational acceleration $\mathbf{g}$, while ∇' is the two-dimensional gradient $(\partial/\partial X, \partial/\partial Y)$.

In Appendix A, it is shown that the above statement holds also for cases such that the temperature field undergoes an axial change, $\partial T/\partial Z \neq 0$. Moreover, in Appendix B, it is shown that the same statement holds not only for a clear fluid, but also for the case of flows in a fluid-saturated porous medium according to the Darcy–Forchheimer model. In the present paper, the term "clear fluid" will be used, following the common practice of treatises on convective flow in porous media, in order to denote the classical Navier–Stokes flow when compared to seepage flow in a porous medium.

The condition for the existence of parallel flow implies that, for a non-vertical duct ($\mathbf{g}' \neq 0$), this special flow solution for the fully developed regime can be found only if the thermal boundary conditions are such that either the vector field $\nabla' T$ is a parallel field with the same direction as the vector $\mathbf{g}'$ or the fluid changes its temperature only in the axial direction, *i.e.* $\nabla' T = 0$. The latter case can hardly be arranged in practice. On the other hand, in the former case, two-dimensional heat transfer occurs in the direction parallel to $\mathbf{g}'$ and in the axial direction. One can easily conclude that, for a vertical duct ($\mathbf{g}' = 0$), a parallel flow solution always exists. Roughly speaking, the necessary condition for parallel flow in a non-vertical duct is that the isotherms on a plane transversal to the flow direction must be parallel straight lines orthogonal to the direction of $\mathbf{g}'$. Such a condition can be hardly fulfilled whenever the duct is not a parallel plane channel. In fact, for a plane channel, the geometry of the boundaries allows one to get parallel straight isotherms in the fluid, for instance, by prescribing uniform temperatures on both the boundary walls (Barletta, 2005). For a different geometry of the duct, the necessary condition for parallel flow can be fulfilled only by prescribing more complicated thermal boundary conditions, as it is shown in the next section with reference to a circular duct.

3. Fully developed flow in an inclined tube

Let us consider a clear fluid flowing in an inclined circular duct having radius R_0 and subjected to a non-axisymmetric wall heat flux. A sketch of the duct and of the origin of the angular coordinate with respect to the gravitational field is given in Fig. 1. As it is shown by this figure, the tilt angle between the duct axis and the direction of the gravitational acceleration is φ and the vector $\mathbf{g}'$ is given by

$$\mathbf{g}' = -(g \sin\varphi)\mathbf{Y}, \tag{1}$$

where $\mathbf{Y}$ is the unit vector in the Y-direction. The incoming wall heat flux is expressed as

$$q_w(\vartheta) = k\left.\frac{\partial T}{\partial R}\right|_{R=R_0} = q_0 \sin\left(\vartheta + \xi\frac{\pi}{2}\right), \tag{2}$$

where (R, ϑ) are two-dimensional polar coordinates, while ξ is a dimensionless switch variable which can be equal either to 0 or 1. On account of Eq. (2), one obtains in this case that the circumferentially averaged wall heat flux vanishes. Moreover, let us assume that the effect of viscous dissipation is negligible and that the flow is fully developed. As a consequence, both the velocity field $\mathbf{U}$ and the temperature field T are invariant in the axial direction, namely $\partial \mathbf{U}/\partial Z = 0$ and $\partial T/\partial Z = 0$. Thus, the governing equations can be written as

$$\nabla' \cdot \mathbf{U}' = 0, \tag{3}$$

$$\varrho_0 \mathbf{U}' \cdot \nabla' \mathbf{U}' = -\varrho_0 \beta (T - T_0)\mathbf{g}' - \nabla' P + \mu \nabla'^2 \mathbf{U}', \tag{4}$$

$$\varrho_0 \mathbf{U}' \cdot \nabla' U_z = -\varrho_0 \beta (T - T_0) g_z - \frac{\partial P}{\partial Z} + \mu \nabla'^2 U_z, \tag{5}$$

$$\varrho_0 c_p (\mathbf{U}' \cdot \nabla' T) = k \nabla'^2 T. \tag{6}$$

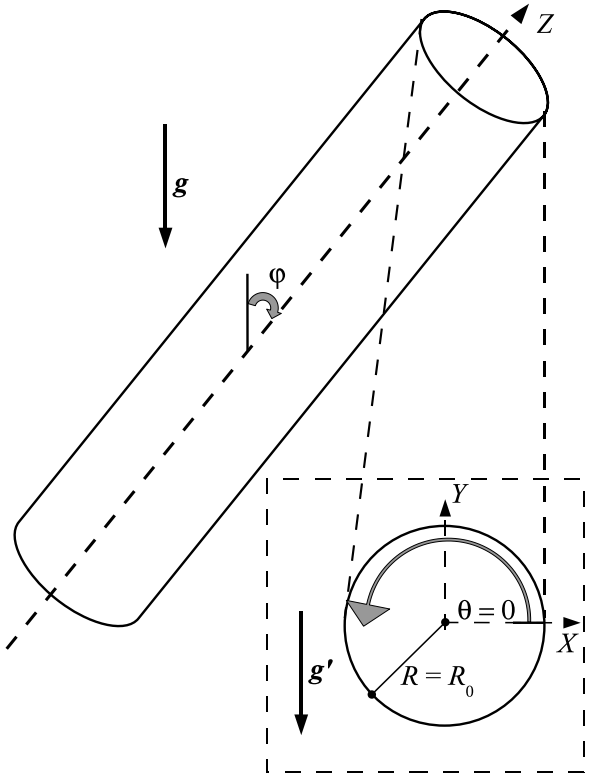

Fig. 1. Sketch of the inclined tube.

Since $\mathbf{U}$ and T do not depend on Z, by differentiating Eqs. (4) and (5) with respect to Z, one obtains

$$\mathbf{V}'\frac{\partial P}{\partial Z}=0, \tag{7}$$

$$\frac{\partial^2 P}{\partial Z^2}=0. \tag{8}$$

Eqs. (7) and (8) allow one to infer that field P can be uniquely represented as

$$P(X,Y,Z)=A(X,Y)+BZ, \tag{9}$$

where B is a constant.

Note that the fields $\mathbf{U}'$ and T can be determined by solving Eqs. (3), (4) and (6). In other words, these fields are not influenced by the axial component U_z. The latter component can be obtained as a last step of the solution procedure, *i.e.* by solving Eq. (5).

Let us introduce the dimensionless quantities,

$$\mathbf{u}'=\frac{2R_0\mathbf{U}'}{\nu},\quad u=\frac{U_z}{U_0},\quad \Theta=k\frac{T-T_0}{q_0R_0},$$
$$x=\frac{X}{R_0},\quad y=\frac{Y}{R_0},\quad r=\frac{R}{R_0},\quad a=\frac{4R_0^2\varrho_0 A}{\mu^2},\quad b=-\frac{2R_0^2B}{\mu U_0},$$
$$Re=\frac{2R_0U_0}{\nu},\quad Gr=\frac{8g\beta q_0R_0^4}{k\nu^2},\quad Pr=\frac{\nu}{\alpha}. \tag{10}$$

The reference temperature T_0 and the reference velocity U_0 are given by

$$T_0=\frac{1}{\pi R_0^2}\int_0^{R_0}\mathrm{d}R\int_0^{2\pi}\mathrm{d}\vartheta RT, \tag{11}$$

$$U_0=\frac{1}{\pi R_0^2}\int_0^{R_0}\mathrm{d}R\int_0^{2\pi}\mathrm{d}\vartheta RU_z. \tag{12}$$

Thus, Eqs. (3)–(6) can be rewritten as

$$\frac{\partial u_x'}{\partial x}+\frac{\partial u_y'}{\partial y}=0, \tag{13}$$

$$u_x'\frac{\partial u_x'}{\partial x}+u_y'\frac{\partial u_x'}{\partial y}=-\frac{\partial a}{\partial x}+2\left(\frac{\partial^2 u_x'}{\partial x^2}+\frac{\partial^2 u_x'}{\partial y^2}\right), \tag{14}$$

$$u_x'\frac{\partial u_y'}{\partial x}+u_y'\frac{\partial u_y'}{\partial y}=\frac{Gr\sin\varphi}{2}\Theta-\frac{\partial a}{\partial y}+2\left(\frac{\partial^2 u_y'}{\partial x^2}+\frac{\partial^2 u_y'}{\partial y^2}\right), \tag{15}$$

$$u_x'\frac{\partial u}{\partial x}+u_y'\frac{\partial u}{\partial y}=\frac{Gr\cos\varphi}{2Re}\Theta+b+2\left(\frac{\partial^2 u}{\partial x^2}+\frac{\partial^2 u}{\partial y^2}\right), \tag{16}$$

$$\frac{Pr}{2}\left(u_x'\frac{\partial\Theta}{\partial x}+u_y'\frac{\partial\Theta}{\partial y}\right)=\frac{\partial^2\Theta}{\partial x^2}+\frac{\partial^2\Theta}{\partial y^2}. \tag{17}$$

On account of Eq. (11), the dimensionless temperature Θ must fulfil the constraint

$$\int_0^1\mathrm{d}r\int_0^{2\pi}\mathrm{d}\vartheta r\Theta=0. \tag{18}$$

3.1. The case $\xi = 0$

If $\xi=0$, a solution of Eqs. (2) and (13)–(17) can be found such that Θ is a function only of the Cartesian coordinate y. Thus, as a consequence of Eq. (1), the condition for parallel flow, $\mathbf{g}'\times\mathbf{V}'T=0$, is fulfilled. One can easily find that

$$\Theta=y=r\sin\vartheta. \tag{19}$$

It must be pointed out that the boundary condition equation (2) with $\xi=0$ is the only one that is compatible with parallel flow for $\varphi\neq 0$. In fact, the parallel flow condition implies that Θ depends only on y and, thus, Eq. (17) can be satisfied in this case only if Θ is a linear function of y. Finally, the constraint equation (18) leads to the conclusion that Θ must be proportional to y and the proportionality constant can be set to 1 by a proper redefinition of q_0. To summarize, parallel flow implies the validity of Eq. (19) and yields the thermal boundary condition equation (2) with $\xi=0$.

Since the flow is parallel, $\mathbf{u}'=0$ and the axial velocity component u fulfils the equation

$$\frac{\partial^2 u}{\partial x^2}+\frac{\partial^2 u}{\partial y^2}+\frac{Gr\cos\varphi}{4Re}\Theta+\frac{b}{2}=0, \tag{20}$$

together with the no-slip condition for $r=1$. In order to determine u, it is convenient to express Eq. (20) in cylindrical polar coordinates

$$\frac{\partial^2 u}{\partial r^2}+\frac{1}{r}\frac{\partial u}{\partial r}+\frac{1}{r^2}\frac{\partial^2 u}{\partial\vartheta^2}+\frac{Gr\cos\varphi}{4Re}r\sin\vartheta+\frac{b}{2}=0. \tag{21}$$

A solution of Eq. (21) that fulfils the no-slip boundary condition

$$u(1,\vartheta)=0, \tag{22}$$

can be sought in the form

$$u(r,\vartheta)=u_1(r)+u_2(r)\sin\vartheta. \tag{23}$$

By substituting Eq. (23) in Eq. (21), one obtains a pair of ordinary differential equations

$$\frac{\mathrm{d}^2u_1}{\mathrm{d}r^2}+\frac{1}{r}\frac{\mathrm{d}u_1}{\mathrm{d}r}+\frac{b}{2}=0, \tag{24}$$

$$\frac{\mathrm{d}^2u_2}{\mathrm{d}r^2}+\frac{1}{r}\frac{\mathrm{d}u_2}{\mathrm{d}r}-\frac{u_2}{r^2}+\frac{Gr\cos\varphi}{4Re}r=0, \tag{25}$$

subjected to the boundary conditions

$$u_1(1)=0=u_2(1). \tag{26}$$

One obtains

$$u_1(r)=\frac{b}{8}(1-r^2), \tag{27}$$

$$u_2(r)=\frac{Gr\cos\varphi}{32Re}r(1-r^2). \tag{28}$$

The value assumed by the constant b can be obtained by imposing the constraint (12), thus yielding

$$b=16. \tag{29}$$

In fact, one gets the same value of b that would be obtained in the case of isothermal Poiseuille flow. This result could have been expected since, as shown by Eq. (23), the buoyancy-induced term $u_2(r)\sin\vartheta$ in the expression of $u(r,\vartheta)$ has a vanishing average value in a duct cross-section. Finally, the transverse distribution of the dimensionless difference between the pressure and the hydrostatic pressure, represented by function $a(r,\vartheta)$, is obtained from Eqs. (14), (15) and (19). These equations yield

$$a(r,\vartheta)=\frac{Gr\sin\varphi}{4}r^2\sin^2\vartheta. \tag{30}$$

Function $a(r,\vartheta)$ can be determined only up to an arbitrary additive constant. In Eq. (30), this constant has been fixed so that $a=0$ for $r=1$ and $\vartheta=0$. Eqs. (19), (23) and (27)–(30) show that the dimensionless solution is governed by parameters Gr and Re as well as by the tilt angle φ and does not depend explicitly on Pr.

3.2. The case $\xi = 1$

If $\xi=1$, on account of Eq. (2), the incoming wall heat flux $q_w(\vartheta)$ is proportional to $\cos\vartheta$, *i.e.* to x. Then, the gradient of T cannot be everywhere parallel to $\mathbf{g}'$ that is directed along the y-axis. One thus concludes, in this case, that it is impossible to have a parallel flow solution, unless $\varphi=0$. For $\varphi=0$, the duct is vertical and $\mathbf{g}'=0$, so that the condition $\mathbf{g}'\times\nabla' T=0$ is satisfied at every point inside the duct. In this case, a simple analytical solution is allowed. Eq. (17) reduces merely to the Laplace equation for Θ. Hence, consistently with the thermal boundary condition, one has

$$\Theta=x=r\cos\vartheta. \tag{31}$$

Following a procedure similar to that described in Section 3.1, one gets

$$u(r,\vartheta)=2(1-r^2)\left(1+\frac{Gr}{64Re}r\cos\vartheta\right),\qquad b=16,\quad a(r,\vartheta)=0. \tag{32}$$

This analytical solution for the vertical duct can be employed as a benchmark to test the numerical solution procedure.

For $\varphi\neq 0$, the non-parallel laminar solution can be obtained numerically by employing a Galerkin finite element method, implemented through the software package Comsol Multiphysics (© Comsol, AB). Although the flow has a 3D nature due to the secondary flow in the xy-plane, the numerical solution, based on Eqs. (13)–(17), is obtained by a purely 2D procedure. Eqs. (13)–(17) reveal that the solution depends on four governing parameters: Re, Gr, Pr and the tilt angle φ. However, one can manage these parameters in order to hide the dependence on φ. In fact, the four governing parameters can be reduced to three by noticing that Eqs. (13)–(17) depend only on

$$\Omega=Gr\sin\varphi,\quad \Lambda=\frac{Gr}{Re}\cos\varphi \tag{33}$$

and Pr. By this optimized parametrization, the limiting case of a vertical duct ($\varphi\to 0$) can be dealt with by taking the limit $\Omega\to 0$. On the other hand, the limiting case of a horizontal duct ($\varphi\to\pi/2$) can be treated by taking the limit $\Lambda\to 0$. Note that the optimized parametrization in terms of Ω and Λ is similar to that introduced by Lavine (1988).

Eq. (32) reveals that, for a vertical duct, the value of b is in any case 16. Therefore, one can base the numerical solution procedure on the guess that $b=16$ for every other possible value of the tilt angle φ or, stated differently, for every possible values of Ω and Λ. The physical meaning of this guess is that the dimensionless axial pressure drop is not influenced by the buoyancy effect. Stated differently, buoyancy does not affect the relation between the mass flow rate and the axial pressure gradient. Thus, this relation is the same that holds in the case of isothermal flow (*Poiseuille flow*). In order to test the reliability of this guess, one prescribes the additional constraint induced by Eq. (12), namely

$$1-\frac{1}{\pi}\int_0^1 \mathrm{d}r\int_0^{2\pi}\mathrm{d}\vartheta ru=0. \tag{34}$$

The method to get the numerical solution involves two steps. First, one solves Eqs. (13)–(15) and (17), that is nothing but a 2D natural convection problem in a circular cavity. Then, one uses the obtained numerical values of $\mathbf{u}'$ and Θ to solve Eq. (16) and thus obtain u. While the fields $\mathbf{u}'$ and Θ depend only on Pr and Ω, the field u depends also on Λ.

One can easily check that, for fixed values of Pr, Eqs. (13)–(17) as well as the boundary conditions prescribed at $r=1$

$$u=0,\quad \frac{\partial\Theta}{\partial r}=\cos\vartheta \tag{35}$$

undergo two fundamental symmetries

$$\begin{pmatrix} x\to -x\\ y\to y\\ \Omega\to-\Omega\\ \Lambda\to-\Lambda\end{pmatrix}\Rightarrow\begin{pmatrix} u'_x\to -u'_x\\ u'_y\to u'_y\\ u\to u\\ \Theta\to-\Theta\\ a\to a\end{pmatrix}, \tag{36}$$

$$\begin{pmatrix} x\to x\\ y\to -y\\ \Omega\to\Omega\\ \Lambda\to-\Lambda\end{pmatrix}\Rightarrow\begin{pmatrix} u'_x\to u'_x\\ u'_y\to -u'_y\\ u\to u\\ \Theta\to-\Theta\\ a\to a\end{pmatrix}. \tag{37}$$

On account of these symmetries, one can restrict the analysis to positive values of both Ω and Λ.

The Nusselt number can be defined as

$$Nu=\frac{2R_0q_0}{k(T_{\max}-T_{\min})}=\frac{2}{\Theta_{\max}-\Theta_{\min}}. \tag{38}$$

It must be pointed out that the maximum and minimum values of Θ always occur on the duct wall $r = 1$. In the cases of parallel flow, defined either by Eqs. (19) and (23)–(30) or by Eq. (32), one has $Nu = 1$. Indeed, the convective heat transfer between the hotter and the cooler parts of the duct wall is entirely due to the secondary flow.

4. Discussion of the results

4.1. The parallel flow case ($\xi = 0$)

The parallel flow solution in the case $\xi = 0$ is represented in Fig. 2. This figure displays plots of $u(r,\vartheta)$ for different values of the governing parameter Λ. It is easily verified that, for $\Lambda = 50$, the z-velocity profile presents a maximum next to 2 and displays a not too marked asymmetry with respect to rotations around the z-axis. In this sense, it does not differ much from the isothermal flow Poiseuille profile. On the other hand, stronger differences appear in the other three plots, where the flow reversal phenomenon arises. The onset of flow reversal takes place next to $(r = 1, \vartheta = 3\pi/2)$, or $(x = 0, y = -1)$. In fact, when $\Lambda > 0$, this position represents the coolest one for upward flow and the hottest one for downward flow. The value of Λ corresponding to the onset of flow reversal can be easily found out by checking the sign of $\partial u/\partial r$ evaluated at $(r = 1, \vartheta = 3\pi/2)$. On account of Eqs. (23), (27), (28), one infers that flow reversal takes place when

$$\Lambda > 64. \tag{39}$$

What happens in the case $\Lambda < 0$ is easily established from Eqs. (23), (27), (28), by noticing that the transformation,

$$\Lambda \to -\Lambda, \quad \vartheta \to \vartheta + \pi, \tag{40}$$

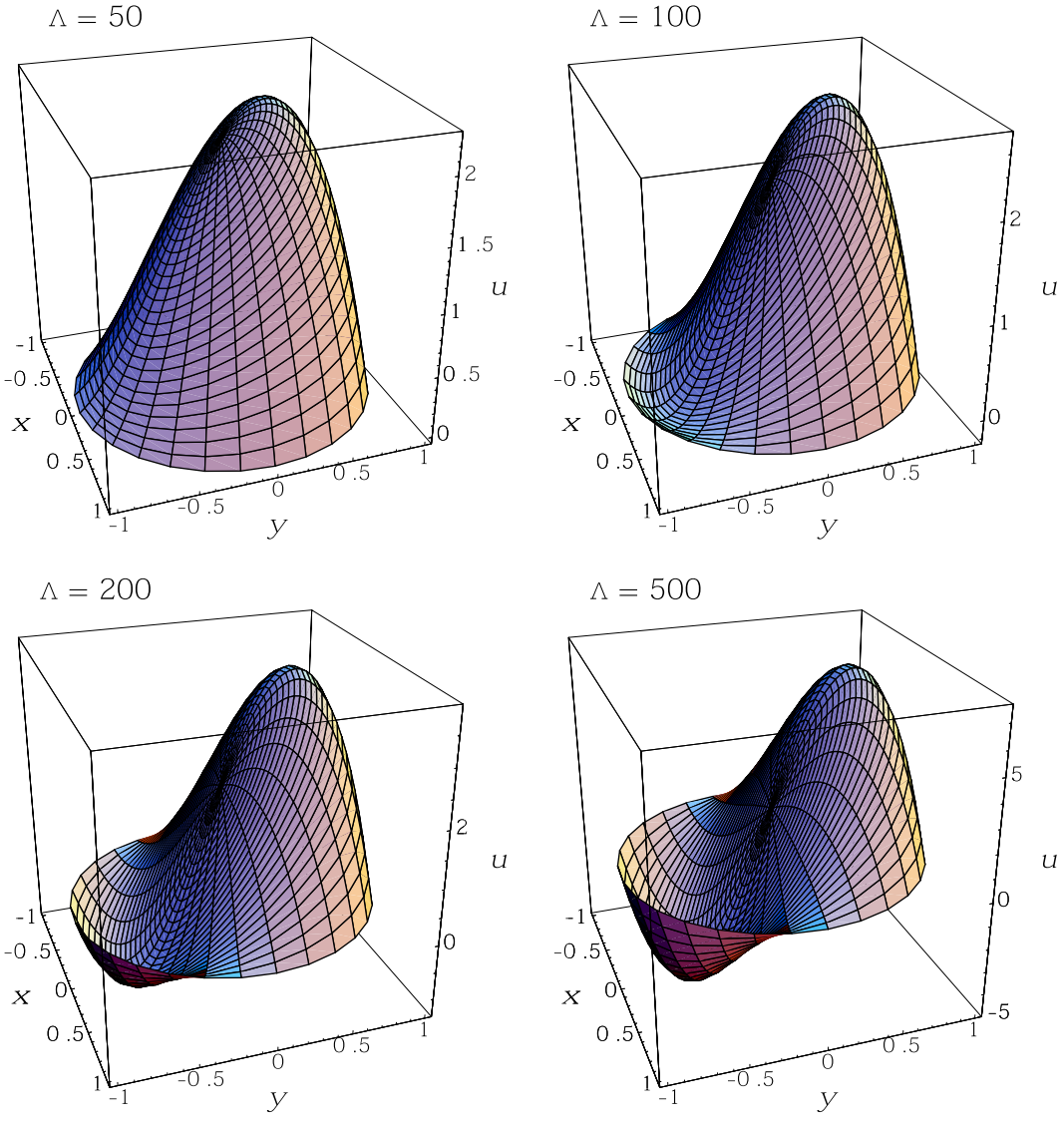

Fig. 2. Case $\xi = 0$. Plots of $u(r,\vartheta)$ for different values of Λ.

leaves u invariant. In particular, this symmetry implies that, for $\Lambda < 0$, the onset of flow reversal takes place next to $(r = 1, \vartheta = \pi/2)$ for

$$\Lambda < -64. \tag{41}$$

4.2. The non-parallel flow case ($\xi = 1$)

The non-parallel flow is studied for a liquid with $Pr = 7$. The computational domain is the dimensionless duct cross-section, *i.e.* the unit circle. Seven structured meshes with an increasing number of quadrangular elements from 1600 to 4900 are defined in this domain in order to test the grid independence. Four quantities are monitored in order to check the grid–independence: the maximum value $u_{\max}$ and the minimum value $u_{\min}$ of u, the value of the Nusselt number Nu and the value of the quantity

$$\varepsilon_k = \frac{1}{\pi}\int_0^1 \mathrm{d}r \int_0^{2\pi} \mathrm{d}\vartheta \frac{r\mathbf{u}'^2}{2}. \tag{42}$$

The latter quantity represents the dimensionless kinetic energy associated with the secondary flow and thus is independent of Λ. The grid independence has been tested with reference to a rather critical flow condition, namely $\Omega = 10^7$ and $\Lambda = 10^4$. The results are compared in Table 1. This table shows that the refinements succeed in driving the numerical simulations to convergence. The parameter most affected by the grid refinement is ε_k. However, the relative change of ε_k between the grid with 3600 elements and that with 4900 elements (36% increase) is 0.03%, while the other quantities $u_{\max}$, $u_{\min}$ and Nu undergo changes around 0.005%. Moreover, the left hand side of Eq. (34) has values lower than 2×10^{-15} in all the cases examined, thus confirming the validity of the guess $b = 16$. As a result of the grid independence test, in the following, the mesh with 4096 elements will be used.

Another check on the reliability of the numerical code is the comparison with the benchmark analytical solution (Section 3.2) in the case of a vertical duct, $\Omega \to 0$. Table 2 refers to different positive values of Λ and displays the calculated values of $u_{\max}$ and $u_{\min}$. As it is shown by this table, the comparison between the numerical solution, obtained for $\Omega = 10^{-7}$, and the benchmark analytical solution reveals a very good agreement, which, in most cases, holds for the first 5 significant digits. Being ε_k independent of Λ, this quantity has a unique value for a vertical duct. Since this special flow is a parallel one, the expected value of ε_k should be zero. In fact, the numerically predicted value of ε_k is rather small: 10^{-19}.

In the following, the cases examined refer to $10^2 \leqslant \Omega \leqslant 10^7$ and $10^{-7} \leqslant \Lambda \leqslant 10^4$. The choice $\Lambda = 10^{-7}$ is a

Table 1
Numerical solution ($\xi = 1$): grid independence test with structured meshes having increasing refinements, for $\Omega = 10^7$, $\Lambda = 10^4$ and $Pr = 7$

Mesh	$u_{\max}$	$u_{\min}$	Nu	ε_k
1600 elements	14.9298	−12.2820	7.45612	56.2996
2025 elements	14.9330	−12.2856	7.45412	56.2186
2500 elements	14.9349	−12.2867	7.45318	56.1743
3025 elements	14.9353	−12.2875	7.45256	56.1484
3600 elements	14.9353	−12.2876	7.45229	56.1323
4096 elements	14.9357	−12.2881	7.45212	56.1237
4900 elements	14.9359	−12.2882	7.45195	56.1149

Table 2
Numerical solution ($\xi = 1$): comparison with the analytical benchmark solution (in *italic*) for $\Omega \to 0$ and $Pr = 7$

Λ	$u_{\max}$	$u_{\min}$
50	2.24683	0.00000
	2.24682	*0.*
100	2.72997	−0.184710
	2.73003	*−0.184723*
200	3.84788	−1.21167
	3.84800	*−1.21168*
500	7.39422	−4.73249
	7.39431	*−4.73249*
1000	13.3852	−10.7200
	13.3855	*−10.7200*
2000	25.4017	−22.7348
	25.4018	*−22.7354*
5000	61.4776	−58.8119
	61.4789	*−58.8123*

The numerical solution is obtained with $\Omega = 10^{-7}$.

Table 3
Numerical solution ($\xi = 1$): values of $u_{\max}$, $u_{\min}$, Nu and ε_k for $Pr = 7$

Ω		$\Lambda = 10^{-7}$	$\Lambda = 10^2$	$\Lambda = 10^3$	$\Lambda = 10^4$
10^2	$u_{\max}$	2.000	2.613	12.05	108.2
	$u_{\min}$	0.000	−0.1030	−9.385	−105.5
	Nu	1.106	1.106	1.106	1.106
	ε_k	0.06339	0.06339	0.06339	0.06339
10^3	$u_{\max}$	2.000	2.258	7.605	63.72
	$u_{\min}$	0.000	0.000	−4.971	−61.08
	Nu	1.705	1.705	1.705	1.705
	ε_k	0.6491	0.6491	0.6491	0.6491
10^4	$u_{\max}$	1.999	2.100	5.059	37.97
	$u_{\min}$	0.000	0.000	−2.440	−35.34
	Nu	2.668	2.668	2.668	2.668
	ε_k	2.608	2.608	2.608	2.608
10^5	$u_{\max}$	2.000	2.048	3.930	26.39
	$u_{\min}$	0.000	0.000	−1.327	−23.76
	Nu	3.854	3.854	3.854	3.854
	ε_k	7.498	7.498	7.498	7.498
10^6	$u_{\max}$	2.001	2.027	3.278	19.49
	$u_{\min}$	0.000	0.000	−0.6907	−16.85
	Nu	5.417	5.417	5.417	5.417
	ε_k	20.54	20.54	20.54	20.54
10^7	$u_{\max}$	2.001	2.016	2.863	14.94
	$u_{\min}$	0.000	0.000	−0.3073	−12.29
	Nu	7.452	7.452	7.452	7.452
	ε_k	56.12	56.12	56.12	56.12

good approximation of the limit $\Lambda \to 0$, *i.e.* the limit of a horizontal duct. Table 3 displays the values of u_{max}, u_{min}, Nu and ε_k. It must be pointed out that both Nu and ε_k, being constructed from the fields $\mathbf{u}'$ and Θ, do not depend on the governing parameter Λ. Table 3 reveals two important features: the Nusselt number and the quantity ε_k are increasing functions of Ω; the onset of flow reversal (negative values of u_{min}) takes place with higher threshold values of Λ as Ω increases. Physically, an increasing value of Ω means a stronger secondary flow. This implies obviously

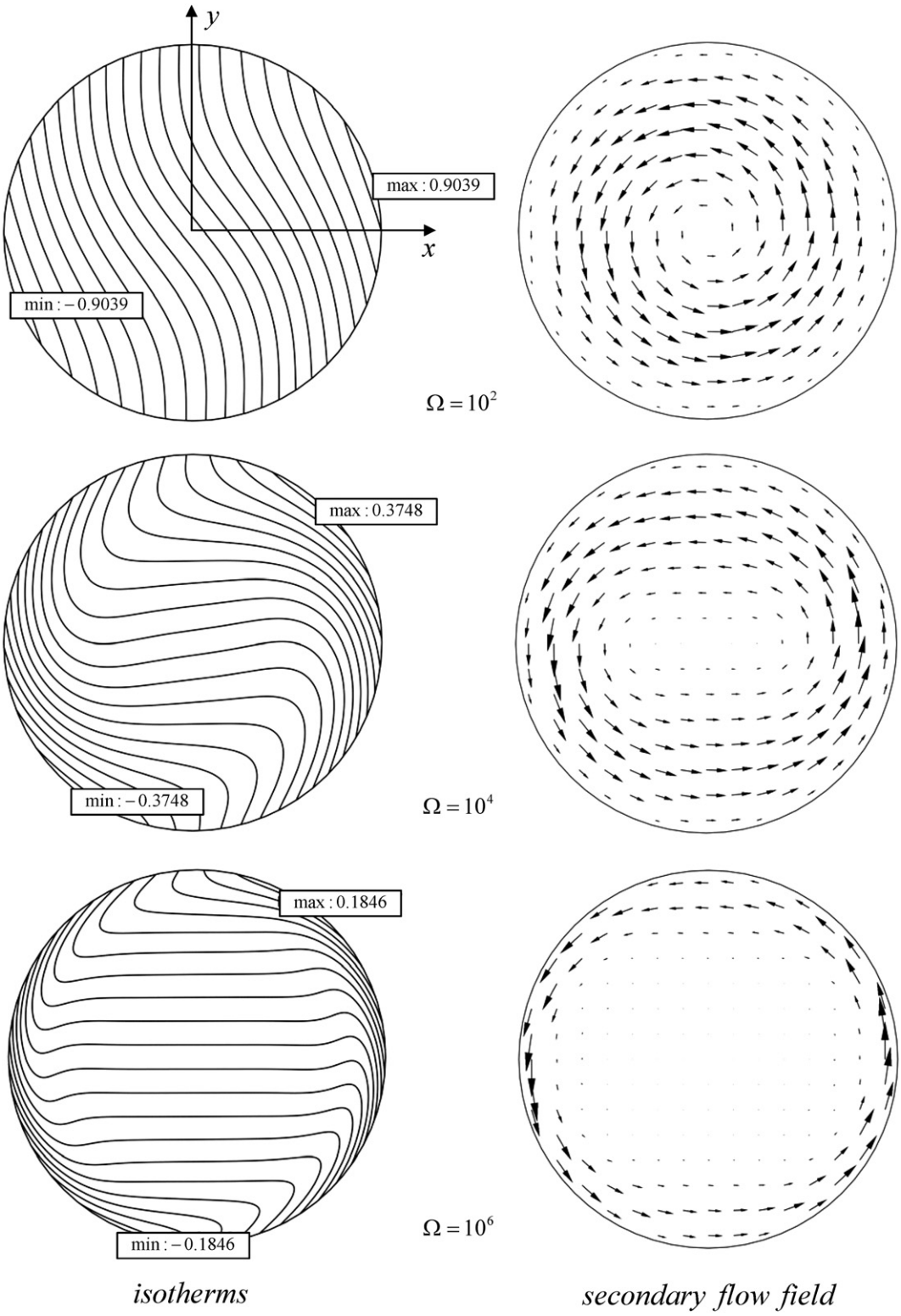

Fig. 3. Case $\xi = 1$. Plots of Θ (isotherms) and $\mathbf{u}'$ (proportional arrow plots) for different values of Ω.

the increasing values of Nu and ε_k, but also the delayed onset of the flow reversal phenomenon, induced by the smaller temperature differences in the duct cross-section. In fact, the flow reversal phenomenon is due to a sufficiently intense buoyancy force that may cause locally a fluid flow in the direction opposite to the mean flow. This sufficiently intense buoyancy force arises when considerable temperature differences are present within the duct cross-section.

Table 3 shows that a horizontal duct ($\Lambda = 10^{-7}$) displays values of $u_{\min}$ and $u_{\max}$ compatible with the Poiseuille velocity profile, whatever is the value of Ω. This means that the coupling between the secondary flow and the axial flow induced by the convective derivative term in Eq. (16) has a

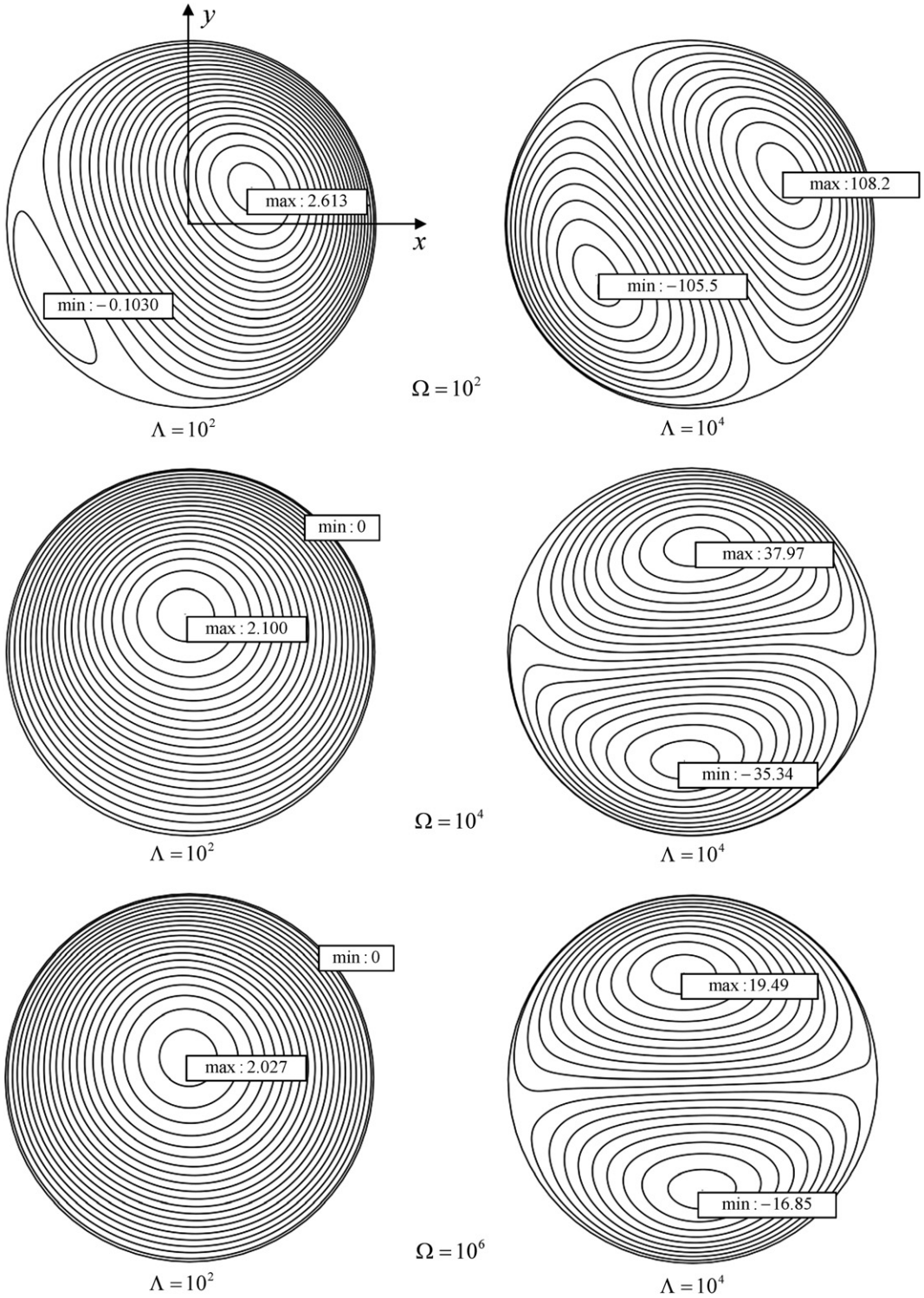

Fig. 4. Case $\xi = 1$. Contour plots of u for different values of Ω and Λ.

negligible effect in this case. For all the values of Ω and Λ considered in Table 3, the left hand side of Eq. (34) has values lower than 4×10^{-15}.

The influence of the parameters Λ and Ω on the velocity and temperature field is also pointed out in Figs. 3 and 4. Fig. 3 shows that, for lower values of Ω, the shape of the isotherms implies a mainly conductive heat transfer in the x-direction, while a dominant thermal stratification in the direction of $\mathbf{g}'$ (y-direction) occurs for higher values of Ω. Fig. 3 shows also that the secondary flow is almost everywhere directed in the ϑ-direction, when Ω is small. On the other hand, as Ω increases, stronger secondary flow occurs in the neighborhood of $\vartheta=0$ and $\vartheta=\pi$, where the maximum incoming and outgoing heat fluxes are prescribed. Fig. 4 reveals that the change in the shape of the isotherms as Ω increases implies a displacement in the positions of the maximum and minimum values of u. For $\Omega=10^2$, the position of the maximum axial velocity corresponds to a value of ϑ intermediate between 0 and $\pi/2$. For $\Omega=10^4$, this position is definitely on the plane $\vartheta=\pi/2$. The latter feature is connected to the thermal stratification in the direction of $\mathbf{g}'$ shown in Fig. 3.

5. Conclusions

Fully developed and laminar mixed convection in an inclined circular tube has been analyzed. The thermal boundary condition prescribed at the duct wall is a non-axisymmetric heat flux varying sinusoidally in the angular direction. It has been shown that this thermal boundary condition has a rather special feature: it can be made compatible with parallel flow by a proper setting of a switch parameter ξ. In fact, parallel flow in an inclined duct different from a parallel plane channel is an exception rather than a rule, and this thermal boundary condition provides precisely the exception. A different tuning of the switch parameter or, stated differently, a $(\pi/2)$-rotation of the wall heat flux distribution restores the rule, *i.e.* non-parallel flow. While, in the parallel flow case, the governing balance equations admit a simple analytical solution, the solution found in the non-parallel flow case has been obtained following a numerical finite element procedure. This numerical solution has been found in the case $Pr=7$, that means, approximately, water at room temperature. The main features of this solution are the following:

- The secondary flow velocity and the temperature field depend on a unique parameter, Ω, whose value is determined by the fluid properties and by the duct radius, by the amplitude of the wall heat flux distribution, q_0, and by the tilt angle, φ. As a consequence, also the Nusselt number depends only on Ω.
- The axial flow velocity component depends on Ω and on another dimensionless parameter, Λ, that is determined by the same quantities involved in the definition of Ω as well as by the mass flow rate.
- The dimensionless pressure drop in the axial direction, b, is not influenced by the buoyancy effect, *i.e.* it is independent of Ω and of Λ. The Nusselt number and the dimensionless kinetic energy ε_k associated to the secondary flow are both increasing functions of Ω.
- The coupling effect between the secondary flow and the axial flow in the special case of a horizontal tube ($\Lambda\to0$) is induced only by the convective derivative term in the axial momentum balance and is rather small. In fact, in all the cases examined, the axial velocity profile for the horizontal tube has negligible differences from the isothermal Poiseuille profile.

Appendix A. Parallel flow for a clear fluid

In the following, it will be shown that the restrictive assumption of an axially invariant temperature field can be released without altering the validity of the necessary condition for parallel flow. Let us consider mixed convection flow of a clear fluid in an inclined duct, such that the cross-section has an arbitrary shape. Let us choose a Cartesian coordinate frame (X, Y, Z) as in Section 2.

In the fully developed region, where

$$\frac{\partial\mathbf{U}}{\partial Z}=0,\quad \frac{\partial\tilde{\varrho}(T,T_0)}{\partial Z}=0, \tag{A.1}$$

the mass, momentum and energy balance equations can be expressed according to the Boussinesq approximation as

$$\boldsymbol{\nabla}'\cdot\mathbf{U}'=0, \tag{A.2}$$

$$\varrho_0\mathbf{U}'\cdot\boldsymbol{\nabla}'\mathbf{U}'=\tilde{\varrho}(T,T_0)\mathbf{g}'-\boldsymbol{\nabla}'P+\mu\nabla'^2\mathbf{U}', \tag{A.3}$$

$$\varrho_0\mathbf{U}'\cdot\boldsymbol{\nabla}'U_z=\tilde{\varrho}(T,T_0)g_z-\frac{\partial P}{\partial Z}+\mu\nabla'^2U_z, \tag{A.4}$$

$$\varrho_0c_p\left[\boldsymbol{\nabla}'\cdot(\mathbf{U}'T)+U_z\frac{\partial T}{\partial Z}\right]=k\left(\nabla'^2T+\frac{\partial^2T}{\partial Z^2}\right)+\mu\Phi. \tag{A.5}$$

In Eqs. (A.1)–(A.5), Φ represents the viscous dissipation function and $\tilde{\varrho}(T,T_0)=\varrho(T)-\varrho_0$, where $\varrho(T)$ is the temperature-dependent mass density evaluated through the equation of state.

If one assumes $\mathbf{U}'=0$, Eq. (A.3) yields

$$\tilde{\varrho}(T,T_0)\mathbf{g}'-\boldsymbol{\nabla}'P=0. \tag{A.6}$$

Since $\mathbf{g}'$ is a constant vector, by evaluating the two-dimensional curl of both sides of Eq. (A.6), one obtains

$$\begin{aligned}0&=\boldsymbol{\nabla}'\times[\tilde{\varrho}(T,T_0)\mathbf{g}'-\boldsymbol{\nabla}'P]=-\mathbf{g}'\times\boldsymbol{\nabla}'\tilde{\varrho}(T,T_0)\\&=-\mathbf{g}'\times\boldsymbol{\nabla}'\varrho(T)=\beta\varrho(T)\mathbf{g}'\times\boldsymbol{\nabla}'T.\end{aligned} \tag{A.7}$$

Eq. (A.7) ensures the validity of the parallel flow condition reported at the beginning of Section 2.

Appendix B. Parallel flow in a Darcy–Forchheimer porous medium

The necessary condition for the occurrence of parallel flow can be stated also in the case of stationary flow in a fluid-saturated porous medium. Let us consider mixed con-

vection flow in an inclined duct filled with a porous medium, such that the cross-section has an arbitrary shape. Let us assume the validity of Darcy–Forchheimer law as well as of the Boussinesq approximation, so that

$$\frac{\mu}{K}\mathbf{U}+\frac{F\varrho_0}{\sqrt{K}}|\mathbf{U}|\mathbf{U}=-\nabla P+\tilde{\varrho}(T,T_0)\mathbf{g}, \tag{B.1}$$

where K is the permeability of the medium and F is Forchheimer coefficient. The velocity $\mathbf{U}$ represents the local average velocity of the fluid often called *Darcy seepage velocity*. The local mass balance still implies that $\nabla\cdot\mathbf{U}=0$ and the local energy balance equation is given by

$$\varrho_0 c_p\mathbf{U}\cdot\nabla T=\hat{k}\nabla^2 T+\frac{\mu}{K}\mathbf{U}^2, \tag{B.2}$$

where $\hat{k}$ is the average thermal conductivity of the fluid-saturated porous medium. As is well known, the term $\mu\mathbf{U}^2/K$ on the right hand side of Eq. (B.2) represents the viscous dissipation contribution.

In the fully developed region defined through Eq. (A.1), the governing equations can be expressed as

$$\nabla'\cdot\mathbf{U}'=0, \tag{B.3}$$

$$\frac{\mu}{K}\mathbf{U}'+\frac{F\varrho_0}{\sqrt{K}}\mathbf{U}'\sqrt{\mathbf{U}'^2+U_z^2}=-\nabla' P+\tilde{\varrho}(T,T_0)\mathbf{g}', \tag{B.4}$$

$$\frac{\mu}{K}U_z+\frac{F\varrho_0}{\sqrt{K}}U_z\sqrt{\mathbf{U}'^2+U_z^2}=-\frac{\partial P}{\partial z}+\tilde{\varrho}(T,T_0)g_z, \tag{B.5}$$

$$\varrho_0 c_p\left[\nabla'\cdot(\mathbf{U}'T)+U_z\frac{\partial T}{\partial Z}\right]=\hat{k}\left(\nabla'^2 T+\frac{\partial^2 T}{\partial Z^2}\right)+\frac{\mu}{K}\left(\mathbf{U}'^2+U_z^2\right). \tag{B.6}$$

It is easily shown that, as in the case of a free fluid, the necessary condition for the occurrence of parallel flow is the local validity of the constraint $\mathbf{g}'\times\nabla' T=0$. The proof coincides with that given in the preceding appendix. Indeed, if the flow is parallel ($\mathbf{U}'=0$), Eq. (B.4) coincides with Eq. (A.6).

References

Aung, W., 1987. Mixed convection in internal flow. In: Kakaç, S., Shah, R.K., Aung, W. (Eds.), Handbook of Single-Phase Convective Heat Transfer. Wiley, New York (Chapter 15).

Barletta, A., 2005. On the existence of parallel flow for mixed convection in an inclined duct. International Journal of Heat and Mass Transfer 48, 2042–2049.

Barletta, A., Zanchini, E., 1999. On the choice of the reference temperature for fully-developed mixed convection in a vertical channel. International Journal of Heat and Mass Transfer 42, 3169–3181.

Barletta, A., Zanchini, E., 2001. Mixed convection with viscous dissipation in an inclined channel with prescribed wall temperatures. International Journal of Heat and Mass Transfer 44, 4267–4275.

Barletta, A., Lazzari, S., Zanchini, E., 2003. Non-axisymmetric forced and free flow in a vertical circular duct. International Journal of Heat and Mass Transfer 46, 4499–4512.

Bühler, K., 2003. Special solutions of Boussinesq-equations for free convection flows in a vertical gap. Heat and Mass Transfer 39, 631–638.

Chamkha, A.J., Groşan, T., Pop, I., 2002. Fully developed free convection of a micropolar fluid in a vertical channel. International Communications in Heat and Mass Transfer 29, 1119–1127.

Lavine, A.S., 1988. Analysis of fully developed opposing mixed convection between inclined parallel plates. Wärme- und Stoffübertragung 23, 249–257.

Magyari, E., 2007. Normal mode analysis of the fully developed free convection flow in a vertical slot with open to capped ends. Heat and Mass Transfer 43, 827–832.

Weidman, P.D., 2006. Convection regime flow in a vertical slot: continuum of solutions from capped to open ends. Heat and Mass Transfer 43, 103–109.